Journal of
Materials in Life Sciences

Vol. 4 No. 2 (2025)

Full Paper

Evaluating Photodegradation Performance of Phosphate Glass Doped with Titanium Dioxide for Water Remediation System

Muhammad Afiq Rosli[a], Siti Norfariza Farhana Mohd Razak[b], Nurhafizah Hasim[b], Fuad Mohamad[a,*]

[a] Department of Chemistry, Faculty of Science, Universiti Teknologi Malaysia, 81310 UTM Johor Bahru, Johor, Malaysia.
[b] Department of Physics, Faculty of Science, Universiti Teknologi Malaysia, 81310 UTM Johor Bahru, Johor, Malaysia.

Article history
Received
30 September 2025
Revised
07 November 2025
Accepted
07 November 2025
Published online
30 November 2025

*Corresponding author
m.fuad@utm.my

Abstract

This study investigates the preparation, characterization and photodegradation properties of TiO_2-doped phosphate glass which focuses on its ability to degrade methyl orange (MO) dye under ultraviolet (UV) light irradiation. The glass system with the composition $(40–x–y)P_2O_5 – 30ZnO – 25Li_2O – 5SrO – (x)CS – (y)TiO_2$) was synthesized using the melt-quenching technique which producing transparent violet glasses with increasing TiO_2 content. Each modifier and dopant in the glass system played a distinct and important role in influencing its physical and chemical behaviour. Zinc oxide (ZnO) enhances the structural integrity and chemical resistance of the glass, lithium oxide (Li_2O) acts as a flux to lower the melting temperature and improve glass conductivity, and strontium oxide (SrO) increases mechanical strength and glass-forming ability. Chitosan (CS), a biopolymer component, helps to promote more surface activity and dye adsorption, while TiO_2 serves as the key photocatalytic dopant responsible for photodegradation activity. Structural characterization using X-ray diffraction (XRD) confirmed the formation of a semi-crystalline structure dominated by the rutile TiO_2 phase. Fourier Transform Infrared (FTIR) spectroscopy revealed the formation of Ti–O–P bonds and the presence of non-bridging oxygens, which indicate the successful incorporation of TiO_2 within the phosphate network. Ultraviolet–Visible Diffuse Reflectance Spectroscopy (UV-Vis DRS) showed a slight narrowing of the optical band gap from 5.41 eV to 5.19 eV with increasing TiO_2 concentration, which suggests enhanced light absorption capability. However, photodegradation experiments showed an unexpected increase in absorbance rather than a decrease, indicating limited photocatalytic efficiency due to uneven TiO_2 dispersion and the dominance of the rutile phase. Future improvements should focus on promoting the anatase phase and optimizing TiO_2 dispersion to enhance the photodegradation performance of phosphate glass for environmental remediation applications.

Keywords Phosphate glass, Titanium dioxide, Photodegradation property, UV irradiation, Methyl orange

1.0 INTRODUCTION

Phosphate glasses have been widely studied due to their tunable properties through the addition of metal oxides, which allow diverse applications such as optical components and biomedical implants [1]. These glasses consist of interconnected PO_4 tetrahedra and are particularly helpful in modification by incorporating other oxides such as lithium oxide (Li_2O), strontium

oxide (SrO) and zinc oxide (ZnO). These modifiers significantly enhance thermal stability, mechanical strength and chemical resistance. For instance, ZnO enhances the durability and chemical resistance of glass [2], Li2O contributes to ionic conductivity and lowers the melting temperature [3], and SrO improves mechanical integrity and glass-forming ability [4, 5]. The combination of these oxides was selected to strengthen the phosphate glass network and ensure that it remains chemically stable under environmental and photocatalytic conditions. Studies comparing borosilicate and phosphate glasses suggest that the chemical composition, particularly phosphorus content plays a crucial role in determining microbial interaction and the overall dissolution behavior of the glass [6].

TiO_2 is widely recognized for its ability to generate reactive oxygen species under ultraviolet (UV) light which makes it an effective photocatalyst for degrading organic pollutants. When doped into phosphate glass, TiO_2 forms Ti–O–P bonds that alter the glass network and affect its optical and structural properties. The resulting material combines the structural stability of phosphate glass with the photocatalytic activity of TiO_2 which makes it suitable for environmental remediation such as wastewater treatment. However, the photodegradation efficiency depends strongly on the TiO_2 phase, with anatase being more active than rutile and its uniform dispersion within the matrix [7].

In this study, chitosan (CS) was introduced as an additional biopolymer modifier to enhance the surface functionality and dye adsorption capability of the glass. The hydroxyl (–OH) and amine ($–NH_2$) groups in chitosan can improve the interaction between the glass surface and organic molecules, which potentially facilitates the photodegradation process of the dye. Despite the known photodegradation properties of TiO_2, its performance when incorporated into phosphate glass matrices remains inconsistent and underexplored. Therefore, this study aims to evaluate the photodegradation performance of phosphate glasses doped with TiO_2 and other modifiers (ZnO, Li_2O, SrO, and CS) prepared using the melt-quenching technique, focusing on the degradation of the methyl orange (MO) dye. Through detailed structural and optical characterization, the relationship between TiO_2 content and photodegradation behaviour is analyzed to assess the potential of these materials for water remediation applications.

2.0 EXPERIMENTAL

2.1 Materials

The raw materials used for synthesizing phosphate glass samples included phosphorus pentoxide (P_2O_5), zinc oxide (ZnO), lithium carbonate (Li_2CO_3), strontium carbonate ($SrCO_3$), chitosan (CS) and titanium dioxide (TiO_2). These were obtained in high purity and used without further purification. TiO_2 was varied in mol% (0 to 1.0%) across six sample compositions and labelled A to F. Additionally, methyl orange (MO) serves as a model pollutant to determine how well these synthetic glass materials degrade under sunlight. A high-pressure mercury lamp was used as the UV light source for photodegradation experiments, and distilled water was used to prepare the MO solution.

2.2 Glass preparation

Phosphate-based glass samples of approximately 15 g each were prepared *via* the conventional melt-quenching method. The glass composition was based on the formula (40 – x – y)P_2O_5 – 30ZnO – 25Li2O – 5SrO – (x)CS – (y)TiO_2. All materials were weighed accurately using an analytical balance according to the desired molar ratios as shown in Table 1. The components were mixed using a Labmill800 milling machine for 30 minutes to ensure homogeneity.

Table 1 : A series of compositions of (40 – x – y) P_2O_5 – 30 ZnO – 25 Li_2O – 5 SrO – (x) CS – (y) TiO_2 glass.

Sample	Composition (mol%)					
	P_2O_5 (40-x-y)	ZnO (30)	Li_2O (25)	SrO (5)	CS (x)	TiO_2 (y)
A	40.0	30.0	25.0	5.0	0	0
B	39.4	30.0	25.0	5.0	0.4	0.2
C	39.2	30.0	25.0	5.0	0.4	0.4
D	39.0	30.0	25.0	5.0	0.4	0.6
E	38.8	30.0	25.0	5.0	0.4	0.8
F	38.6	30.0	25.0	5.0	0.4	1.0

The mixed batch was preheated in a furnace at 280°C for 1 hour to remove moisture. The preheated powder was then melted at 1000°C in an alumina crucible for 30 minutes. The resulting molten glass was poured onto a stainless-steel

plate preheated to 280°C and immediately transferred to an annealing furnace at 300 °C for 3 hours to relieve internal stress. The samples were then allowed to cool slowly to room temperature overnight.

2.3 Fourier Transform Infrared (FTIR) Spectroscopy

Fourier Transform Infrared (FTIR) spectroscopy was carried out to obtain the transmission and absorption spectra of the powdered samples in the infrared region. The analysis was performed using a Perkin Elmer Spectrum GX FTIR Spectrometer at the FTIR Laboratory, Department of Chemistry, Faculty of Science, Universiti Teknologi Malaysia (UTM), Johor. The samples were analyzed in powder form using the KBr pellet method over a spectral range of 4000–650 cm^{-1} with a resolution of 4 cm^{-1}. Each spectrum was collected by averaging 100 scans at room temperature to enhance the signal-to-noise ratio. All spectra were corrected for background interference.

2.4 X-ray Diffraction (XRD)

An X-ray diffractometer by Rigaku SmartLab operating at 40 kV and 30 mA is used to observe the amorphous structure of the glasses and the crystalline structure of the glass ceramics. Data were collected using Ni-filtered Cu Kα radiation over a 2θ range of 10°–100° in flat plate geometry at a step size of 0.019967° and a count time of 0.1 second.

2.5 Ultraviolet-Visible Diffuse Reflectance Spectroscopy (UV-Vis DRS)

Ultraviolet-Visible Diffuse Reflectance Spectroscopy (UV-Vis DRS) was employed to investigate the optical properties and estimate the band gap energies of the powdered glass samples. The measurements were carried out using a Shimadzu UV-3101PC scanning spectrophotometer (Kyoto, Japan) equipped with an integrating sphere accessory for diffuse reflectance mode. Powdered samples were placed directly into the sample holder, and air was used as the reference material. The reflectance spectra were recorded over a wavelength range of 200 to 800 nm.

2.6 Photodegradation of Methyl Orange (MO) using UV-Vis Spectroscopy

Photodegradation performance was tested by immersing each glass sample in a 20 mg/L MO solution adjusted to pH 2–3 with HCl. After establishing adsorption equilibrium in the dark for 30 minutes, samples were irradiated with a high-pressure mercury UV lamp. Absorbance was measured at 506 nm using a Shimadzu UV-2501PC spectrophotometer. The decrease in absorbance indicates dye degradation.

$$Percent\ degradation\ (\%) = \left(\frac{Abs_I - Abs_F}{Abs_F}\right) \times 100\%$$

Where, Abs_I = initial absorbance of MO at $\lambda = 506\ nm$, and Abs_F = final absorbance of MO at $\lambda = 506\ nm$.

3.0 RESULTS AND DISCUSSION

3.1 Prepared Glass Samples

Phosphate glass samples with varying TiO_2 content were successfully synthesized using the melt-quenching technique. Visually, the base sample A (0% TiO_2) was transparent while increasing TiO_2 content caused the glass to turn progressively violet, likely due to the partial reduction of Ti^{4+} to Ti^{3+} during melting, as shown in Figure 1 [7].

This colour change confirms the incorporation of TiO_2 into the glass matrix. Density measurements revealed a consistent increase from 6.266 to 10.618 g/cm^3 with rising TiO_2 content, suggesting tighter atomic packing [14]. Meanwhile, the molar volume decreased from 14.977 to 8.725 cm^3/mol, which indicates reduced free volume, which may limit light penetration and restrict photodegradation activity [8][9].

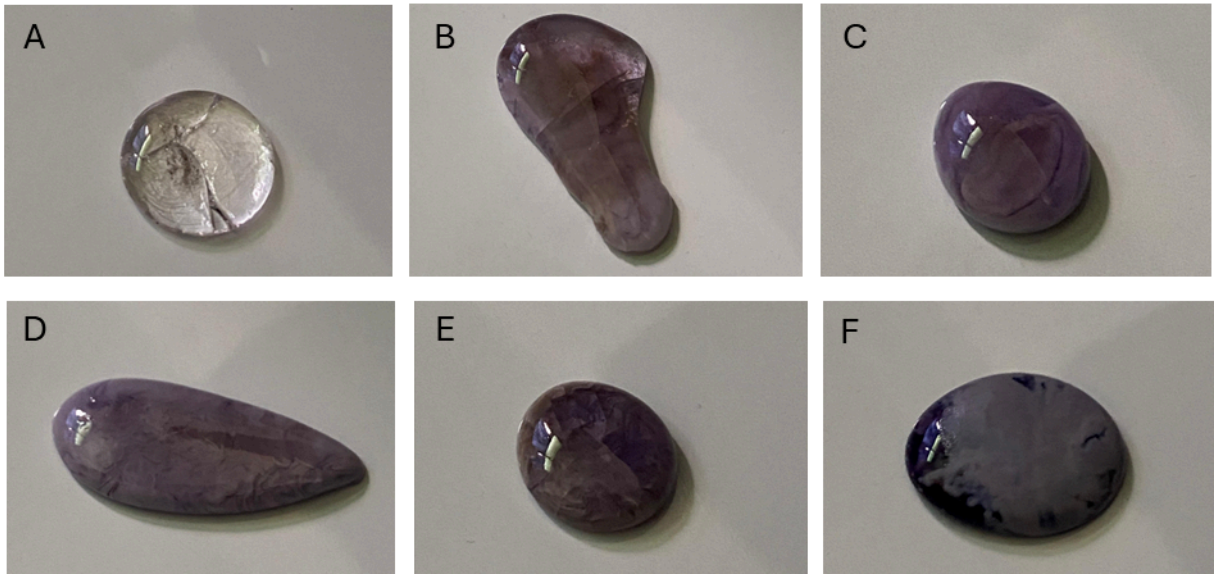

Figure 1: Glass sample prepared with varying concentration of TiO_2 with (a) 0.0%, (b) 0.2%, (c) 0.4%, (d) 0.6%, (e) 0.8% and (f) 1.0% TiO_2. The glass colour becomes progressively darker with increasing TiO_2 content.

3.2 Characterization of the Glass

3.2.1 Fourier Transform Infrared (FTIR) Analysis

FTIR spectroscopy was used to identify the structural units and vibrational changes in the glass network. Absorption bands at 735–746 cm^{-1} and 940–950 cm^{-1} were attributed to the symmetric and asymmetric stretching of P–O–P bridges, respectively [7]. With increasing TiO_2 content, a shift to higher wavenumbers was observed, indicating the formation of Ti–O–P bonds and the disruption of phosphate chains. The PO_2^- stretching band (1200–1222 cm^{-1}) became more intense, signifying increased formation of non-bridging oxygen and enhanced glass depolymerization [10, 11].

Broad O–H stretching bands between 3300–3500 cm^{-1} appeared in TiO_2 and chitosan-containing samples (B–F), confirming minor moisture adsorption. This observation is consistent with the hygroscopic nature of phosphate glasses and the presence of hydroxyl groups in chitosan [2]. The infrared absorption spectra of the glasses were recorded in the range of 4000–650 cm^{-1} at room temperature, as illustrated in Figure 2. The absorption peak positions and their proposed assignments are summarized in Table 2 to facilitate the interpretation of infrared spectra.

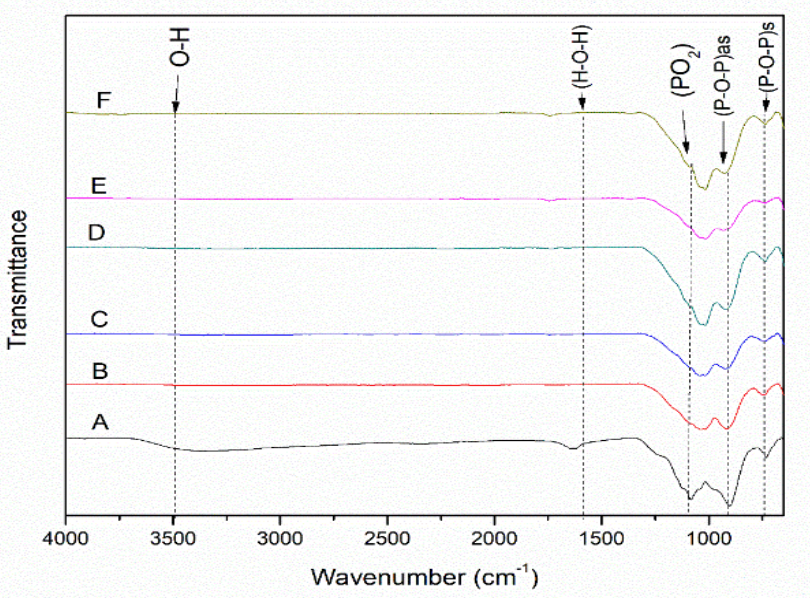

Figure 2: FTIR spectra of phosphate glass with varying concentration of TiO_2 with A (0.0% TiO_2), B (0.2% TiO_2), C (0.4% TiO_2), D (0.6% TiO_2), E (0.8% TiO_2), and F (1.0% TiO_2).

Table 2: FTIR peaks positions of the glass system

Sample	IR Band (cm^{-1})				
A	735	940	1200	1630	3410
B	738	943	1206	1632	3422
C	740	945	1210	1635	3435
D	742	946	1214	1636	3440
E	744	948	1218	1638	3450
F	746	950	1222	1640	3465
Peak Assignments	Symmetric stretching vibration of P-O-P bridges	Asymmetric stretching of P – O – P bridges	PO_2^- (non-bridges oxygen)	H – O – H bending vibration	O–H stretching

3.2.2 X-Ray Diffraction

XRD analysis confirmed that Sample F (1.0% TiO_2) displayed a semi-crystalline structure with nanocrystalline TiO_2 phases embedded in an amorphous matrix. As summarized in Table 3, the sample exhibited distinct peaks corresponding to both anatase and rutile phases of TiO_2. The presence of anatase was confirmed by peaks at 25.10° and 48.82°, which closely match the reference peaks at 25.28° and 48.34° (JCPDS 21-1272). Meanwhile, peaks at 27.37°, 36.24° and 41.40° correspond well with rutile TiO_2 (JCPDS 21-1276).

The predominance of rutile-related peaks suggests that rutile is the major crystalline phase, while anatase is present in smaller quantities. Anatase, which is known for higher photodegradation efficiency due to its higher conduction band and slower charge recombination, was present only in small quantities [7]. The average crystallite size of TiO_2 was estimated at 11.3 nm using the Williamson–Hall method.

Minor peaks were also observed at 31.8° and 25.5°, indicating the presence of ZnO and Sr3(PO4)2, respectively, supporting partial crystallization of secondary phases during glass formation [12]. The XRD pattern of Sample F, as shown in Figure 3, displays a sharp peak confirming the presence of nanocrystalline phases embedded within the glassy matrix, indicating a semi-crystalline structure.

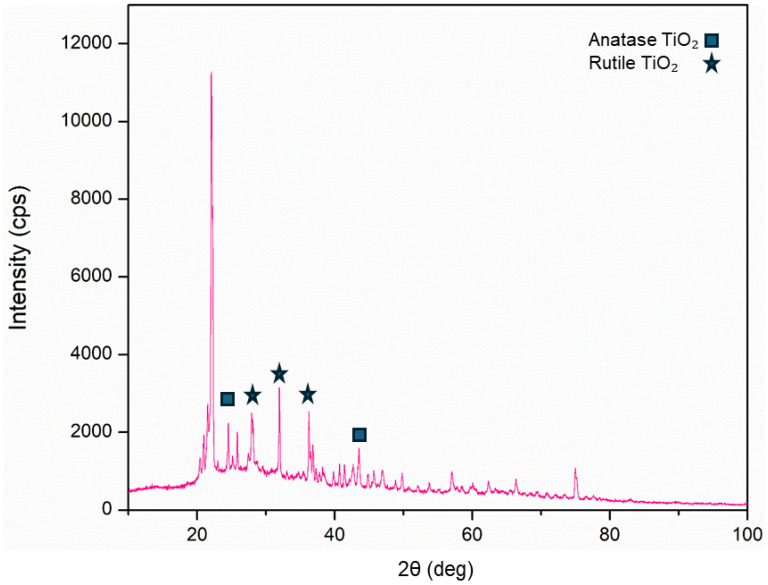

Figure 3 : XRD diffractograms of sample F with 1.0% TiO_2.

2θ (deg)

Table 3 : Crystalline Phases in the Glass Sample by XRD Peak Matching with JCPDS References.

2θ (Sample)	Phase	**2θ (Reference)**
25.10	Anatase TiO_2	25.28 (JCPDS 21-1272)
27.37	Rutile TiO_2	27.33 (JCPDS 21-1276)
36.24	Rutile TiO_2	36.09 (JCPDS 21-1276
41.40	Rutile TiO_2	41.23 (JCPDS 21-1276
48.82	Anatase TiO_2	48.34 (JCPDS 21-1272)

3.2.3 Ultraviolet-Visible Diffuse Reflectance Spectroscopy (UV-Vis DRS)

Diffuse reflectance measurements were conducted to evaluate the optical band gap of phosphate glass samples with varying TiO_2 concentrations. The reflectance spectra, shown in Figure 4, reveal an absorption edge in the UV region for all samples. TiO_2 is a wide bandgap semiconductor (~3.2 eV) that primarily absorbs UV light [13]. As the TiO_2 concentration increased from 0.0% to 1.0%, a gradual shift of the absorption edge toward longer wavelengths (lower photon energies) was observed, indicating increased optical absorption in the near-UV region.

The corresponding Tauc plots in Figure 5 were used to estimate the optical band gaps by extrapolating the linear portion of the $(\alpha h\nu)^2$ versus $h\nu$ curves. The calculated band gap values decreased slightly from approximately 5.41 eV for the undoped glass (Sample A) to 5.19 eV for the 1.0% TiO_2-doped glass (Sample F). This progressive reduction in band gap energy suggests that TiO_2 incorporation introduces localized states near the conduction band, thereby facilitating lower-energy electronic transitions and enhancing near-UV absorption [4]. To evaluate the overall impact of TiO_2 doping, the band gap energy was calculated for all six samples. Table 4 presents the TiO_2 concentration and corresponding estimated band gap values.

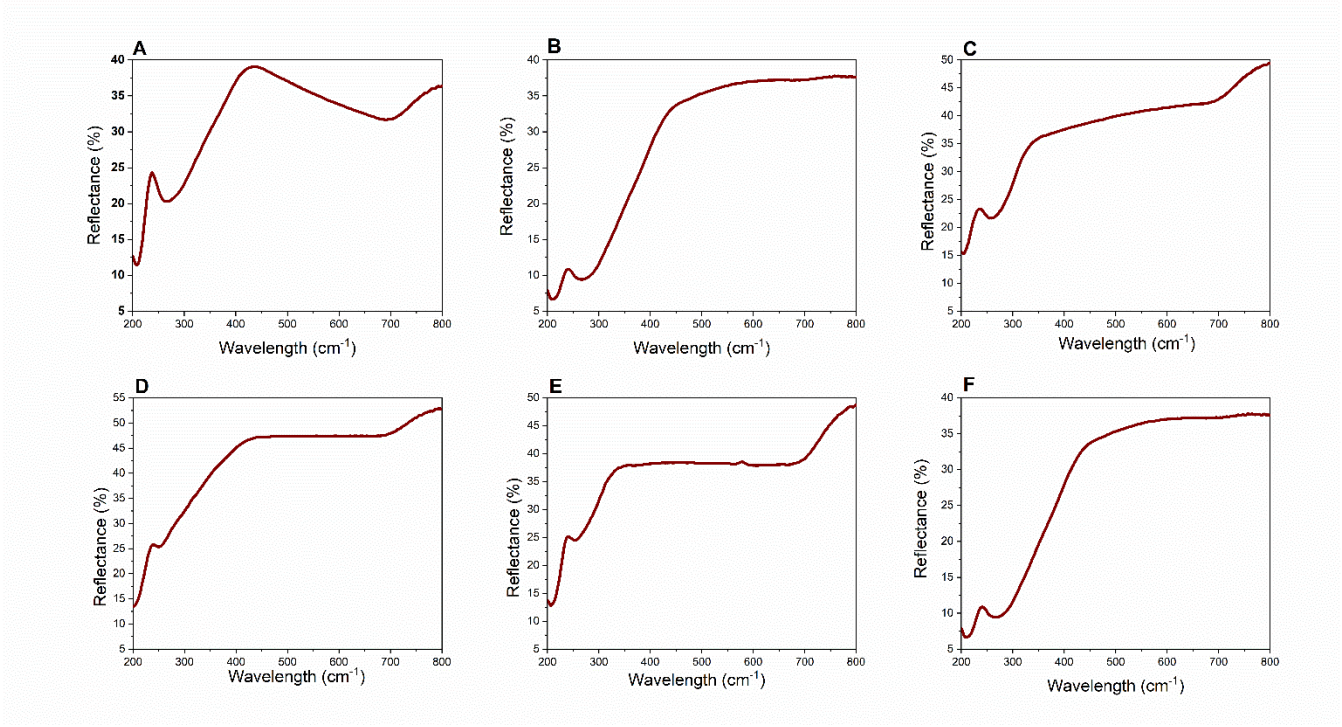

Figure 4 Reflectance spectra of phosphate glass samples with varying TiO_2 concentrations (A: 0.0%, B: 0.2%, C: 0.4%, D: 0.6%, E: 0.8%, and F: 1.0%).

3.2.4 Photodegradation Properties

The photodegradation performance of the TiO_2-doped phosphate glass samples was evaluated using methyl orange (MO) as a model dye under ultraviolet (UV) irradiation. The experiment involved immersing each glass sample in an acidic MO solution (pH 2–3, 20 mg/L) and exposing it to UV light from a 39W mercury lamp while the distance of the sample from the UV light was approximately 5cm. Acidic conditions were maintained to keep MO in its protonated (azo) form, which exhibits strong

absorbance at 506 nm to ensure consistent interaction with the catalyst surface [14]. Absorbance at 506 nm was measured before and after UV exposure to monitor the degradation behaviour of the dye.

All samples were first immersed in the MO solution in the dark for 30 minutes to establish adsorption-desorption equilibrium. The initial absorbance values recorded in the dark showed slight variations among the samples, ranging from 0.685 to 0.920, which are A1 = 0.716, B1 = 0.685, C1 = 0.708, D1 = 0.735, E1 = 0.901 and F1 = 0.920. These results show that only a small amount of MO was adsorbed onto the glass surfaces, with slightly higher adsorption in samples containing more TiO_2 (E and F) due to their rougher surfaces and extra active sites from TiO_2 [15, 16].

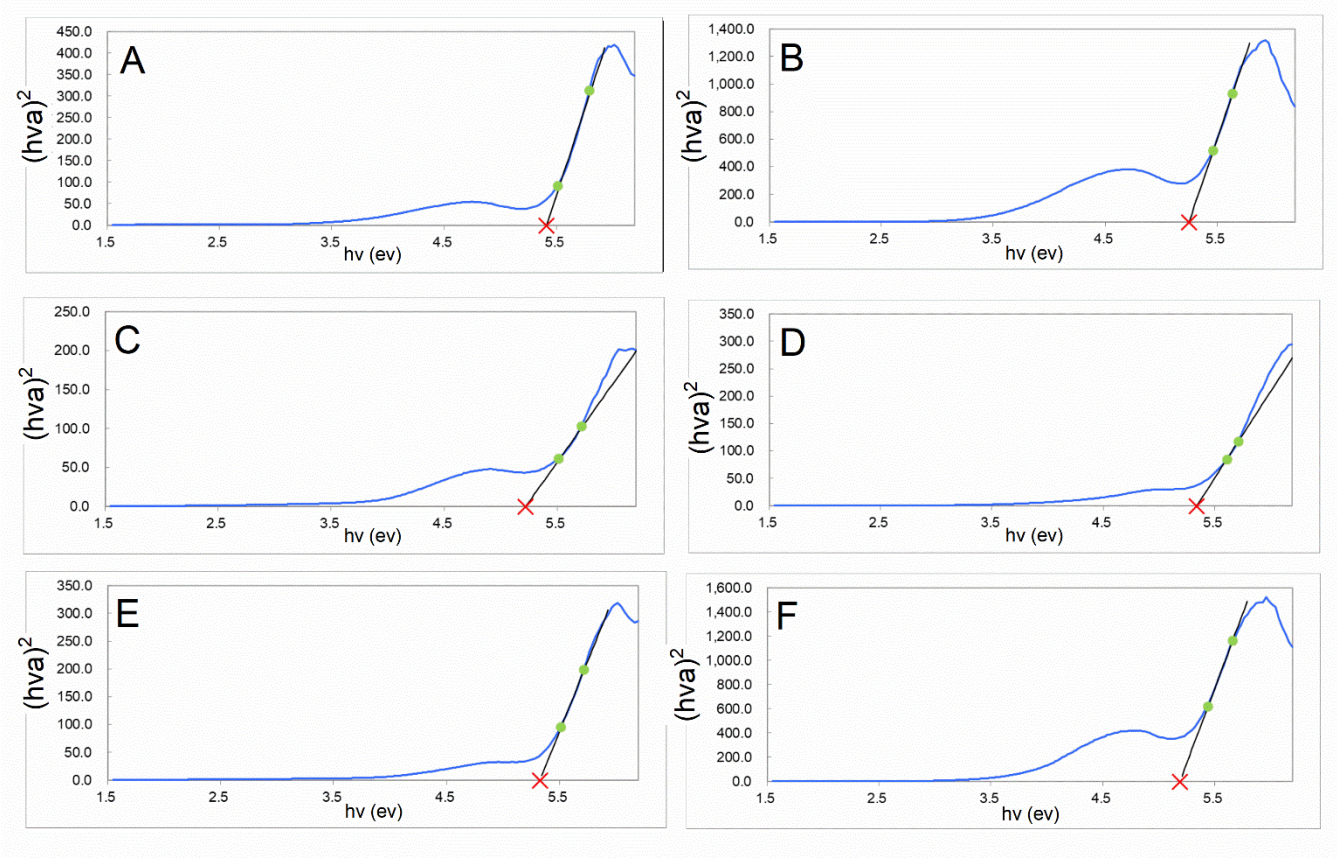

Figure 5 : Tauc plots of phosphate glass samples with varying TiO_2 concentrations (A: 0.0%, B: 0.2%, C: 0.4%, D: 0.6%, E: 0.8%, and F: 1.0%).

Table 4: Band Gap Energy (eV) vs Composition TiO_2 (%)

Sample	Composition TiO_2 (%)	Band gap (eV)
A	0	5.41
B	0.2	5.25
C	0.4	5.22
D	0.6	5.34
E	0.8	5.33
F	1.0	5.19

After 2 hours of UV irradiation, the absorbance values increased across all samples, A2 = 0.853, B2 = 0.836, C2 = 0.848, D2 = 0.853, E2 = 1.049 and F2 = 1.059 as shown in Figure 6. The increase in absorbance rather than a decrease suggests that no significant photodegradation occurred under UV exposure. For the undoped glass (Sample A, 0% TiO_2), only minor changes in absorbance were recorded, confirming its limited interaction with MO. In contrast, Samples E and F (0.8–1.0% TiO_2) exhibited the highest post-irradiation absorbance, which indicates stronger dye adsorption on the surface rather than actual degradation.

The data suggest that TiO_2 incorporation increased the surface affinity of the glass toward MO but failed to facilitate effective photodegradation [3, 17]. This could be attributed to insufficient surface exposure of TiO_2 as the melt-quenching process likely embedded the photocatalyst within the bulk of the glass [18, 19].

Overall, the poor photodegradation performance observed can be ascribed to the dominance of less active TiO_2 phases, inadequate TiO_2 dispersion and limited UV light accessibility [20]. Future work should aim to enhance anatase phase formation and surface exposure, possibly by optimizing synthesis conditions or incorporating TiO_2 more strategically onto the glass surface. As shown in Table 5, the calculated degradation percentages were all negative which ranged from -13.13% to -18.05%. This clearly confirms that instead of breaking down, the MO concentration slightly increased after UV exposure.

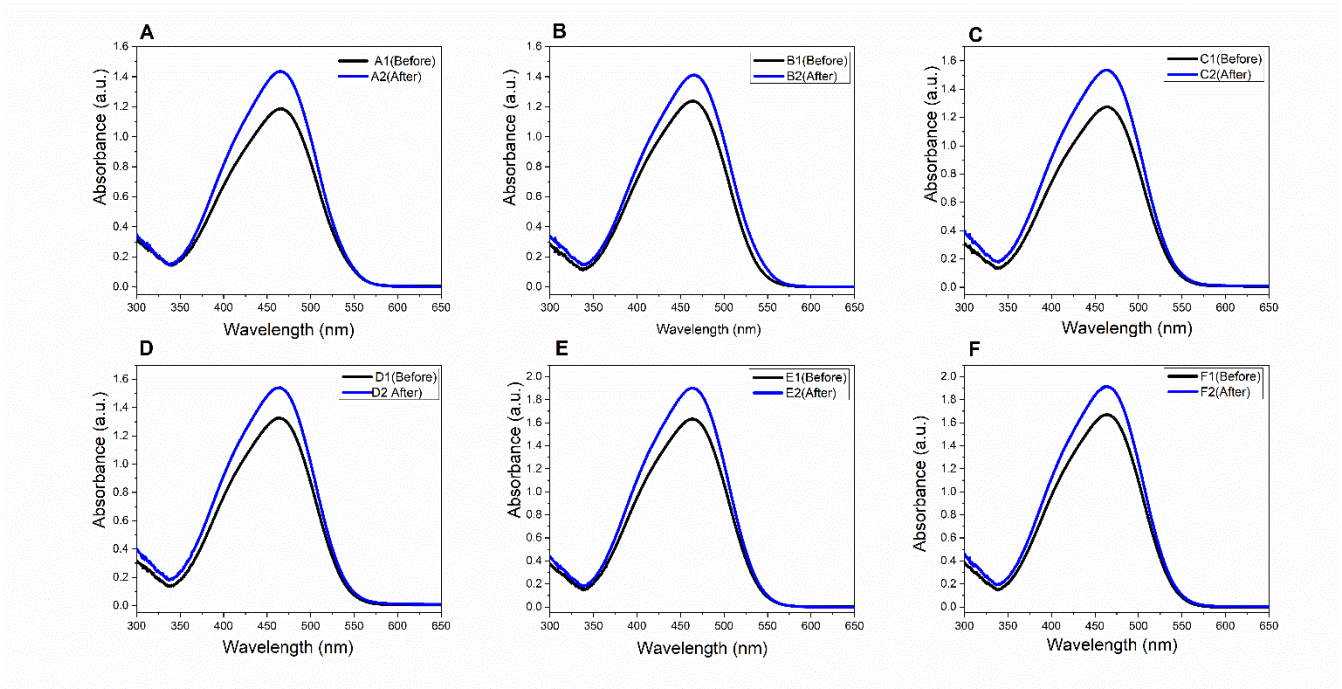

Figure 6 UV Spectra of MO solutions with the presence of TiO_2-doped phosphate glass sample concentrations (A: 0.0%, B: 0.2%, C: 0.4%, D: 0.6%, E: 0.8%, and F: 1.0%).

Table 5 : Photodegradation performance of phosphate glass samples under UV irradiation

Sample	Before UV	After UV	Degradation of Methyl Orange (%)
A	0.716	0.853	-16.07
B	0.685	0.836	-18.05
C	0.708	0.848	-16.51
D	0.735	0.853	-13.84
E	0.901	1.049	-14.11
F	0.920	1.059	-13.13

4.0 CONCLUSION

Phosphate glass doped with titanium dioxide (TiO_2) was successfully synthesized via the melt-quenching method and characterized using FTIR, XRD and UV-Vis DRS techniques. Structural analysis confirmed the formation of Ti–O–P bonds and increased non-bridging oxygens, while XRD revealed a semi-crystalline structure with a dominant rutile phase and minimal anatase content. UV-Vis DRS analysis showed a slight reduction in the optical band gap from 5.41 eV to 5.19 eV with increasing TiO_2 concentration. Despite these changes, photodegradation experiments indicated poor photodegradation activity, with increased absorbance of methyl orange under UV light. To enhance performance, future studies should focus on promoting anatase crystallinity, improving TiO_2 distribution and exploring co-doping or post-synthesis treatments. These improvements could help realize the potential of TiO_2-doped phosphate glass for photocatalytic applications in environmental remediation.

Acknowledgment

The authors would like to acknowledge all individuals who have supported this research, especially the Department of Chemistry and Department of Physics, Faculty of Science, Universiti Teknologi Malaysia, for providing laboratory facilities and

technical assistance. This work is part of a research project R.J130000.7854.5F635 (PY/2023/02164) - Fundamental Research Grant Scheme (FRGS) and [Q.J091600.3100.00A37] - University Industry Research Lab (UIRL), PPMU, UTM under Dana Universiti Penyelidikan (Caj Analisis Makmal) (NHH, SNFAR) and Matching Grant UTM-UI with cost centre of Q.J130000.3054.04M61 (MAR, FM).

References

[1] Abdelghany, A. M., El-Damrawi, G., Oraby, A. H., & Madshal, M. A. (2018). Optical and FTIR structural studies on CoO-doped strontium phosphate glasses. Journal of Non-Crystalline Solids, 499(July), 153–158. https://doi.org/10.1016/j.jnoncrysol.2018.07.022

[2] Alemu, D., Getachew, E., & Mondal, A. K. (2023). Study on the physicochemical properties of chitosan and their applications in the biomedical sector. International Journal of Polymer Science, 2023, Article 5025341.https://doi.org/10.1155/2023/5025341

[3] Alves, R., Junior, H. P. A., Cartaxo, J. M., Rodrigues, A. M., Neves, G. A., & Menezes, R. R. (2021). Use of nanostructured and modified TiO_2 as a gas sensing agent. Cerâmica, 67(383), 316–326. https://doi.org/10.1590/0366-69132021673833128

[4] Aouadi, A., Hamada Saud, D., Rebiai, A., Achouri, A., Benabdesselam, S., Mohamed Abd El-Mordy, F., Pohl, P., Ahmad, S. F., Attia, S. M., Abulkhair, H. S., Ararem, A., & Messaoudi, M. (2024). Introducing the antibacterial and photocatalytic degradation potentials of biosynthesized chitosan, chitosan–ZnO, and chitosan–ZnO/PVP nanoparticles. Scientific Reports, 14(1), Article 14753. https://doi.org/10.1038/s41598-024-65579-z

[5] Bouabdalli, E. M., El Jouad, M., Touhtouh, S., & Hajjaji, A. (2023). First investigation of the effect of strontium oxide on the structure of phosphate glasses using molecular dynamics simulations. Computational Materials Science, 220(February), 112068. https://doi.org/10.1016/j.commatsci.2023.112068

[6] C., L., Thorpe, R., Crawford, R. J., Hand, J. T., Radford, C. L., Corkhill, C. I., Pearce, J. J., Neeway, A. E., Plymale, A. A., Kruger, K., Morris, C., Boothman, J. R., & Lloyd, J. R. (2023). Microbial interactions with phosphorus-containing glasses representative of vitrified radioactive waste. Journal of Hazardous Materials. https://doi.org/10.1016/j.jhazmat.2023.132667

[7] Barba-Nieto, I., Caudillo-Flores, U., Fernández-García, M., & Kubacka, A. (2020). Sunlight-operated TiO_2-based photocatalysts. Molecules, 25(17), 4008.

[8] Brogi, S. R., Charrière, B., Gonnelli, M., Vaultier, F., Sempéré, R., Vestri, S., & Santinelli, C. (2020). Effect of UV and visible radiation on optical properties of chromophoric dissolved organic matter released by Emiliania huxleyi. Journal of Marine Science and Engineering, 8(11), Article 888. https://doi.org/10.3390/jmse8110888

[9] Nesbitt, H. W., Dean, P. A., Henderson, G. S., & Bancroft, G. M. (2025). Effects of Na_2O on the volumetric properties of sodic glasses, including structural relaxation. Chemical Geology, 695, 123081. https://doi.org/10.1016/j.chemgeo.2025.123081

[10] Bouabdalli, E. M., El Jouad, M., Touhtouh, S., Sadek, O., & Hajjaji, A. (2022). Structural studies on varied concentrations of europium doped strontium phosphate glasses. Materials Today: Proceedings, 66, 349–352. https://doi.org/10.1016/j.matpr.2022.05.450

[11] Nesbitt, H. W., Dean, P. A., Bancroft, M., & Henderson, G. S. (2021). Effects of electronegativities and charge delocalization on Q^2 Raman shifts of alkaline- and alkaline earth-bearing glasses and metasilicate crystals. American Mineralogist, 107(11), 2044–2053. https://doi.org/10.2138/am-2022-8172

[12] Bouabdalli, E. M., El Jouad, M., Gaumer, N., Siniti, M., Touhtouh, S., & Hajjaji, A. (2023). Structural, physical, thermal and optical spectroscopy studies of the europium doped strontium phosphate glasses. Inorganic Chemistry Communications, 151(February), 110563. https://doi.org/10.1016/j.inoche.2023.110563

[13] Hossain, R., Uddin, M. A., & Khan, M. A. (2023). Mechanistic understanding in manipulating energetics of TiO_2 for photocatalysis. The Journal of Physical Chemistry C, 127(23), 10897–10912. https://doi.org/10.1021/acs.jpcc.2c06981

[14] You, K., Kwon, O., & Kim, D. (2023). Effects of protonation and polar solvation on the molecular properties of methyl orange: A density functional theory study. Bulletin of the Korean Chemical Society, 44(6), 523–527. https://doi.org/10.1002/bkcs.12682

[15] Lee, B. J., Yoon, Y. S., & Lee, M. B. (2020). Optical and surface characteristics of TiO_2 thin films deposited using RF magnetron sputtering. New Physics: Sae Mulli, 70(7), 556–562. https://doi.org/10.3938/npsm.70.556

[16] Hossain, M. F., Pervez, M. S., & Nahid, M. A. I. (2020). Influence of film thickness on optical and morphological properties of TiO_2 thin films. Emerging Materials Research, 9(1), 1–5. https://doi.org/10.1680/jemmr.17.00085

[17] Sui, W., Zheng, J., Pittman, C. U., Bensalah, N., Wu, M., & Zhao, Y. (2013). Properties of a three-dimensionally ordered macro-mesoporous carbon-doped TiO_2 composite catalyst. Functional Materials Letters, 7(1), 1350068. https://doi.org/10.1142/S1793604713500689

[18] Machinin, A. M., Awang, A., & Pien, C. F. (2023). Physical and optical traits of tellurite glass: Effect of bimetallic TiO_2/Au nanoparticles. Journal of Ovonic Research, 19(3), 321–329. https://doi.org/10.15251/jor.2023.193.321

[19] Tian, N. P., Peng, Z., Du, X., Zheng, W., & Yuan, J. (2019). The effect of melting temperature on coloration of TiO_2–BaO–SiO_2 glass. Glass Physics and Chemistry, 45(3), 208–212. https://doi.org/10.1134/S1087659619030143

[20] Yamazaki, S., Takaki, D., Nishiyama, N., & Yamazaki, Y. (2020). Factors affecting photocatalytic activity of TiO_2. In Elsevier eBooks (pp. 23–38). https://doi.org/10.1016/B978-0-12-819000-5.00003-5